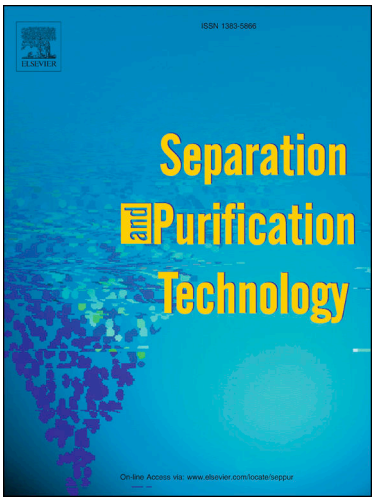

Optimization of the supercritical fluid extraction of *Quercus cerris* cork towards extraction yield and selectivity to friedelin

M.M.R. de Melo, P.G. Vieira, Ali Şen, H. Pereira, I. Portugal, C.M. Silva

PII: S1383-5866(19)34267-4
DOI: https://doi.org/10.1016/j.seppur.2019.116395
Reference: SEPPUR 116395

To appear in: *Separation and Purification Technology*

Received Date: 18 September 2019
Revised Date: 26 November 2019
Accepted Date: 4 December 2019

Please cite this article as: M.M.R. de Melo, P.G. Vieira, A. Şen, H. Pereira, I. Portugal, C.M. Silva, Optimization of the supercritical fluid extraction of *Quercus cerris* cork towards extraction yield and selectivity to friedelin, *Separation and Purification Technology* (2019), doi: https://doi.org/10.1016/j.seppur.2019.116395

Optimization of the supercritical fluid extraction of *Quercus cerris* cork towards extraction yield and selectivity to friedelin

M.M.R. de Melo[1], P.G. Vieira[1], Ali Şen[2], H. Pereira[2], I. Portugal[1], C.M. Silva[1]*

[1] CICECO – Aveiro Institute of Materials, Department of Chemistry, University of Aveiro, Aveiro 3810-193, Portugal

[2] Centro de Estudos Florestais, Instituto Superior de Agronomia, Universidade de Lisboa, Tapada da Ajuda, 1349-017 Lisboa, Portugal

Abstract:

Optimization of the supercritical fluid extraction of *Quercus cerris* cork was carried out using Box-Behnken design of experiments and response surface methodology (RSM). The optimized process variables were temperature (T: 40, 50 and 60 ℃), ethanol content (EtOH: 0.0, 2.5 and 5.0 wt.%) and CO_2 flow rate (Q_{CO_2}: 5, 8 and 11 $g\,min^{-1}$). The studied responses were total extraction yield (η_{Total}), friedelin concentration of the extract ($C_{Friedelin}$), and selectivity towards friedelin ($\alpha_{F,nF}$). The linear effect of EtOH was by far the most influent operating condition (Pareto analysis) and the highest yield (η_{Total}= 2.2 wt.%) was attained with 5.0 wt.% EtOH. The RSM model estimates maximum friedelin concentration in the extracts (38.2 wt.%) to occur without cosolvent (0 wt.% EtOH) for the lowest T (40 ℃) and Q_{CO_2} (5 $g_{CO_2}\,min^{-1}$). As per selectivity, the experimental $\alpha_{F,nF}$ values were always higher than 1.0 and reached 3.1 (at 50 ℃, 5 wt.% EtOH, 11 $g_{CO_2}\,min^{-1}$). Altogether, these results suggest friedelin can be selectively removed from *Quercus cerris* cork by supercritical fluid extraction within the range of experimental conditions studied.

Keywords: Cork, Design of Experiments, Friedelin, *Quercus cerris*, Selectivity.

1. Introduction

Cork is a very important natural material due to its unique properties such as compressibility, impermeability and low thermal conductivity. The cork oak tree (*Quercus suber*) is the primary source for the production of cork stoppers for the wine industry [1,2]. Nevertheless, many other products are attainable from cork such as insulation and surfacing materials [2] or even sorbents used for the removal of heavy metals from wastewaters [1,3]. Some of these alternative applications are based on cork residues, which are produced in large amounts by the cork industries. For example, cork powder represents 30 % of the raw material processed for cork stoppers production [4].

In the case of the Turkey oak tree (*Quercus cerris*), presently the plant is merely used as fuel for energy production [5] despite its valuable fraction of cork. In order to boost the economic exploitation of this species, in recent years the extraction of chemicals from *Q. cerris* cork has been studied with a special focus on friedelin ($C_{30}H_{50}O$), one of the most important extractives. Friedelin, whose basic information is presented in Figure 1, is a pentacyclic triterpene ketone, solid at room conditions, and with an estimated polar surface of 17 Å^2. It exhibits antioxidant features useful for retarding the progression of some oxidative stress-related diseases [6] and with promising bioactive properties such as analgesic, antipyretic, anti-inflammatory and anti-tumor [7, 8].

An European patent application has been filled for a process of extraction and purification of friedelin from cork and cork-derived materials [9]. The proposal involves the use of noxious organic solvents such as chloroform, methylene chloride or diethyl ether, and enforces the evaporation of large amounts of such solvents before a crystalized extract is ultimately obtained [9]. Supercritical fluid extraction (SFE) is a greener alternative successfully applied for the extraction of multiple vegetable matrices [10–12]. Typically, supercritical carbon dioxide (SC-CO_2) is used as the non-

polar/weakly polar extraction solvent due to its mild critical temperature and pressure ($T_c = 31.1$ ºC and $P_c = 73.8$ bar) and nontoxicity. In addition, the properties of SC-CO_2 can be tuned introducing small quantities of a more polar cosolvent (*e.g.*, ethanol) to favor the uptake of more polar compounds. The general advantages of SFE using SC-CO_2 are the prompt separation of the solvent at the end of the process, from both the solid matrix and the produced extract, and the possibility of recycling and reusing it multiple times.

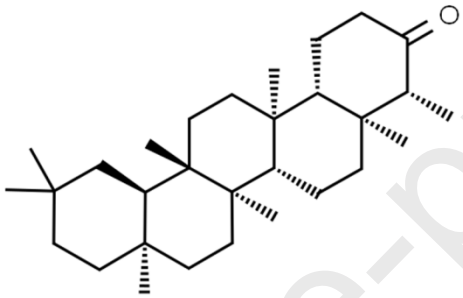

Molecular Formula:	$C_{30}H_{50}O$
Melting Point:	263 °C
Predicted Boiling Point:	447 °C
Predicted Polar Surface Area:	17 Å^2
Predicted Molar Volume:	443.0 ± 3.0 cm^3 mol^{-1}

Figure 1 – Molecular structure of friedelin and basic physicochemical properties of the compound. Melting point: experimental database; boiling point: adapted Stein & Brown method; surface area and molar volume: ACD/Labs Percepta Platform - PhysChem Module. All data were retrieved from [31].

Şen *et al.* [5] obtained friedelin rich extracts (concentrations of 30.4-40.6 wt.%) from *Q. cerris* cork using SC-CO_2 at 300 bar and 40-80 ºC. Later, de Melo *et al.* [13] assessed the influence of the cork particle size and the concentration of ethanol (cosolvent) on total extraction yield (η_{Total}) and friedelin extraction yield ($\eta_{\text{Friedelin}}$). In the case of particle size, intermediate granulometries (from 60-80 mesh to 20-40 mesh) were shown to be more advantageous than smaller (> 80 mesh) or coarser particles [13]. Moreover,

although the use of 5 wt.% of ethanol can enhance η_{Total} up to three times (reaching 2.3 wt.%), intermediate contents of cosolvent (*ca.* 2.5 wt.%) are preferable in terms of selectivity to friedelin, otherwise an abundant removal of non-target extractives prevails [13]. A clear improvement of selectivity towards friedelin was also detected for higher extraction times.

At the current point of research, it is necessary to study the influence of the SFE operating conditions upon the extraction of *Q. cerris* cork, namely the SC-CO_2 flow rate and the extraction temperature in combination with the cosolvent (ethanol) content. For this purpose, a combined approach based on Design of Experiments (DoE) and Response Surface Methodology (RSM) was implemented to model the individual and crossed influence of all these parameters towards the optimum operation region for enhanced production of friedelin-enriched extracts.

2. Materials and methods

2.1 Chemicals and biomass samples

Ethanol (purity 99.5 %) and dichloromethane (purity 99.98 %) were supplied by Fisher Scientific (Leicestershire, United Kingdom). CO_2 (purity 99 %) was supplied by Air Liquide (Algés, Portugal). Friedelin (95 % purity), chlorotrimethylsilane (TMSCl, purity 99 %), N,O-bis(trimethylsilyl)trifluoroacetamine (BTSFA, purity 98 %) and pyridine (purity 99.5 %) were supplied by Sigma Aldrich (Deutschland).

Q. cerris bark was obtained from Kahramanmaras, Turkey, and was granulated with a hammer-type industrial mill. The resulting granules were separated by density difference in distilled water, with 10 min mixing time. The floating fraction of cork-enriched granules (subsequently named cork) was dried, grinded and sieved. The 20-40 mesh (0.42-0.84 mm) fraction was used for it comprises a trade-off between the

negative industrial impact of grinding and the expectable yield and selectivity gain performances [13]. The moisture content of the biomass (5.6 wt.%) was measured by drying *ca.* 3 g of cork at 60 ℃ during 24 h.

2.2 Soxhlet and batch solid-liquid extractions

Soxhlet extractions were carried out during 8 h using *ca.* 3 g of 20-40 mesh *Q. cerris* cork and 120 mL of dichloromethane or ethanol as solvent.

Furthermore, batch solid-liquid extractions (SLE) were performed at room temperature (23 ºC) using sealed beakers containing *ca.* 3 g of 20-40 mesh *Q. cerris* cork and 30 mL of dichloromethane or ethanol (*i.e.,* 1:10 w/v ratio), during 24 h with periodic shaking (manually). In both processes, the solid was filtered off and the extract samples were dried, weighed and analyzed by gas chromatography coupled to mass spectroscopy (GC-MS).

2.3 Gas chromatography coupled to mass spectroscopy (GC-MS)

For GC-MS analysis *ca.* 20 mg of each dried extract was converted into trimethylsilyl (TMS) derivatives [14] as follows: the sample was first dissolved in 250 µL of pyridine containing 1 mg of tetracosane followed by the addition of 250 µL of BTSFA and 50 µL of TMSCl to promote the conversion of compounds with hydroxyl and carboxyl groups into TMS ethers and esters, respectively. The ensuing mixture was maintained at 70 ℃ for 30 minutes [15] and analyzed in duplicate using tetracosane as internal standard. The reported results are the average of these measurements.

The analysis was performed in a Shimadzu GCMS-QP2010 Ultra coupled with an auto-sampler and equipped with a DB-1 J&W capillary column (30 m × 0.32 mm i.d., 0.25 µm film thickness). Helium was the carrier gas (40 cm s^{-1}) and the chromatographic

conditions were as follows [5]: initial temperature of 80 ℃ for 5 min; heating rate at 4 ℃ min^{-1}; final temperature of 300 ℃ for 30 min; injector temperature of 280 ℃; transfer-line temperature of 290 ℃; split ratio of 1:50. The MS was operated in the electron impact mode with electron impact energy of 70 eV and data was collected at a rate of 0.1 scans s^{-1} over a range of m/z of 33-750. The ion source was maintained at 250 ℃.

2.4 Supercritical fluid extraction

SFE experiments were performed in a 0.5 L capacity Speed™ apparatus (Applied Separations, USA) whose flowsheet is illustrated in Figure 2. Operation starts with the pressurization of liquid CO_2 by a cooled liquid pump, followed by mixing with the cosolvent (ethanol) and heating the mixture to reach the supercritical state. Then the supercritical solvent enters the bottom of the extractor previously loaded with biomass (*ca.* 45 g of cork per run). After the predefined extraction time the outlet stream is depressurized through a heated back pressure regulator valve (BPR) and bubbled into a cooled vessel partially filled with ethanol. Therefore, the spent CO_2 is vented to the atmosphere and the solutes remain trapped in ethanol, which is removed by evaporation. Finally, the extract samples are weighed and analyzed by GC-MS.

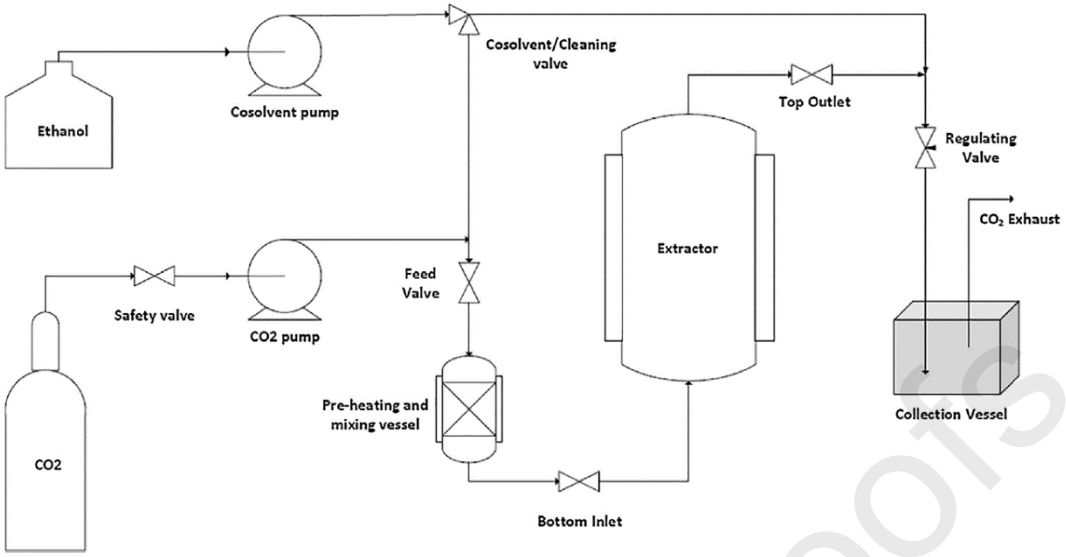

Figure 2 - Simplified flowsheet of the SFE unit. Retrieved from [32].

In the case of SFE with ethanol addition, the cosolvent was introduced using a liquid pump (LabAlliance Model 1500) coupled to the CO_2 line before the mixing/pre-heating vessel.

Total extraction yield (η_{Total}), friedelin concentration in the extracts ($C_{\text{Friedelin}}$), and selectivity to friedelin ($\alpha_{\text{F,nF}}$) were investigated as process responses. Their determination was performed according to the following relations:

$$\eta_{\text{Total}}(\text{wt.\%}) = \frac{w_{\text{extract}}}{w_{\text{biomass}}} \times 100 \quad (1)$$

$$\eta_{\text{Friedelin}}(\text{wt.\%}) = \frac{w_{\text{Friedelin}}}{w_{\text{biomass}}} \times 100 \quad (2)$$

$$\eta_{\text{non-Friedelin}}(\text{wt.\%}) = \eta_{\text{Total}} - \eta_{\text{Friedelin}} \quad (3)$$

$$C_{\text{Friedelin}}(\text{wt.\%}) = \frac{w_{\text{Friedelin}}}{w_{\text{extract}}} \times 100 \quad (4)$$

$$\alpha_{\text{F,nF}} = \frac{\eta_{\text{Friedelin}} \times [X_{0,\text{non-Friedelin}} - \eta_{\text{non-Friedelin}}]}{\eta_{\text{non-Friedelin}} \times [X_{0,\text{Friedelin}} - \eta_{\text{Friedelin}}]} \quad (5)$$

where w_{extract} is the mass of dry extract, w_{biomass} is the mass of cork used in each experiment, and $w_{\text{Friedelin}}$ is the mass of extracted friedelin (quantified by GC-MS). The attainable contents of friedelin ($X_{0,\text{Friedelin}}$) in the pristine raw material are 0.46 and 0.74

wt.% for SFE with pure and ethanol modified SC-CO_2, respectively. For the same fluid types, the SFE attainable contents of non-friedelin ($X_{0,\text{Friedelin}}$) are 1.70 and 3.40 wt.%, respectively.

2.5 Design of Experiments (DoE) and Response Surface Methodology (RSM)

Response surface methodology (RSM) is useful for process development and optimization especially when the response (dependent variable) is influenced by several factors (independent variables) [16]. The main objective is to establish a relationship between the response and the operating variables in order to optimize the response(s) towards a desirable outcome. Typically, RSM involves the fitting of empirical models relating the studied factors and their interactions with the experimental response(s). The first stage of RSM involves the realization of a series of experiments, which can be planned by a design of experiments (DoE), which allows precise and complete information to be obtained from a minimum number of assays. This methodology has been successfully applied to SFE of natural matrices, including spent coffee grounds [17], *Cannabis sativa* L. seeds [18], *Eucalyptus globulus* bark [15], *Diospyros kaki L.* [19], *Magnolia officinalis* bark [20], tomato skins [21], *Corydalis yanhusuo* rhizomes [22], and others [10].

In this work, the influence of the operating conditions was studied using a Box-Behnken design (BBd) of three factors and three levels, totalizing 15 experiments randomly performed in order to minimize unknown and uncontrollable effects (nuisance factor). The chosen factors and respective levels were temperature (T = 40, 50 and 60 ℃), ethanol concentration (EtOH = 0.0, 2.5 and 5.0 wt.%), and CO_2 flow rate (Q_{CO_2}= 5, 8

and 11 g $\min^{-1}$) as systematized in Table 1. The remaining operating conditions were fixed, namely: pressure ($P = 300$ bar), extraction time ($t = 8$ h), and particle size, ($d_p = 20 - 40$ mesh). The independent variables were codified as follows:

$$X_{\mathrm{k}} = \frac{x_{\mathrm{k}} - x_0}{\Delta x_{\mathrm{k}}} \tag{6}$$

where X_k is the codified value of the independent variable x_k, x_0 is its real value at the central point, and Δx_k is the step change between levels for the k variable.

Experimental SFE results analyzed by RSM are usually well described by a second order polynomial function such as:

$$\mathrm{Y} = \beta_0 + \sum_{\mathrm{i}=1}^{3} \beta_{\mathrm{i}} \mathrm{X}_{\mathrm{i}} + \sum_{\mathrm{i}=1}^{3} \beta_{\mathrm{ii}} \mathrm{X}_{\mathrm{i}}^2 + \sum_{\mathrm{i}=1}^{3} \sum_{\mathrm{j}>\mathrm{i}}^{3} \beta_{ij} X_i X_j \tag{7}$$

where Y is the studied response (whether η_{Total}, $C_{\mathrm{Friedelin}}$ or $\alpha_{\mathrm{F,\,nF}}$), β_0 is a constant, β_{i} are model coefficients associated to linear effects, β_{ii} are coefficients linked to quadratic effects, and β_{ij} are coefficients for interaction effects.

STATISTICA software (version 5.1, StatSoft Inc., Tulsa, USA) was used in this work. An analysis of variance (ANOVA) was employed to assess the statistically significant factors and interactions using Fisher's test and its associated probability p(F). In addition, t-tests were applied to judge the significance of the fitted coefficients of each model. The coefficient of determination, R^2, the adjusted coefficient of determination, R^2_{adj}, and the average absolute relative deviation ($AARD$) were used to evaluate the goodness of fit of the regressed model [23]. The coefficients of determination were calculated as follows:

$$R^2 = 1 - \frac{SS_E}{SS_T} \tag{8}$$

$$R^2_{\text{adj}} = 1 - \frac{\frac{SS_E}{n-p-1}}{\frac{SS_T}{n-1}} = 1 - \frac{n-1}{n-p-1}(1-R^2) \quad (9)$$

where SS_E represents the sum of squares error, SS_T represents the total sum of squares, n and p represent the total number of assays and the model degrees of freedom, respectively. In turn, the $AARD$ was determined as follows:

$$\text{AARD}(\%) = \frac{100}{n}\sum_{j=1}^{n}\left|\frac{y_j^{\text{calc}} - y_j^{\text{exp}}}{y_j^{\text{exp}}}\right| \quad (10)$$

where n is the number of data points, and y_j^{calc} and y_j^{exp} are the calculated and experimental responses (η_{Total}, $C_{\text{Friedelin}}$, $\alpha_{\text{F,nF}}$), respectively.

3. Results and discussion

3.1 Analysis of experimental results

The experimental results (η_{Total}, $C_{\text{Friedelin}}$, and $\alpha_{\text{F,nF}}$) for the Soxhlet, SLE and SFE assays are presented in Table 2 along with the corresponding experimental conditions. The SFE η_{Total} values ranged from 0.6 wt.% in run SFE5 [50 ℃, 0.0 wt.% EtOH, 5 g_{CO_2} min^{-1}] to 2.2 wt.% in both runs SFE11 [50 ℃, 5.0 wt.% EtOH, 11 $g_{CO_2}\text{min}^{-1}$] and SFE15 [60 ℃, 5.0 wt.% EtOH, 8 $g_{CO_2}\text{min}^{-1}$]. In turn, Soxhlet and SLE extractions with dichloromethane yielded 4.3 and 1.5 wt.%, respectively. The equivalent assays for ethanol yielded 7.2 and 2.2 wt.%, respectively, thus evidencing a much greater margin for the uptake of polar extractives.

The reproducibility of the SFE assays can was determined for each response through

runs SFE7 to SFE9, which are replicates of the central point of the studied experimental space. The experimental errors thus obtained amounts 12.1 % for η_{Total}, 7.0 % for $C_{\text{Friedelin}}$, and 15.4 % for $\alpha_{\text{F,nF}}$.

The best yields for SFE (runs SFE11 and SFE15, Table 2) are almost half of the Soxhlet yield (4.3 wt.%), 1.5 times higher than for SLE (1.5 wt.%) and 65 % of the maximum SFE attainable yield ($X_0 = 3.4$ wt.% for SFE using SC-CO_2 with 5 wt.% EtOH). In this respect, it is worth mentioning that Soxhlet extractions are favored by both the multiple loads of fresh solvent generated in the unit and by the extraction temperature, which is close to the solvent boiling point (39.6 °C for dichloromethane, or 78.4 ºC for ethanol) while for SLE it was the room temperature (*ca.* 23 ºC).

Friedelin concentration ($C_{\text{Friedelin}}$) in the supercritical extracts ranged from 25.3 wt.% (SFE7: 50 ℃, 2.5 wt.% EtOH, 8 $g_{CO_2}\text{min}^{-1}$) to 36.2 wt.% (SFE2: 40 ℃, 2.5 wt.% EtOH, 5 $g_{CO_2}\text{min}^{-1}$), meaning that the SFE assays scored higher than Soxhlet ($C_{\text{Friedelin}}$ = 24.2 wt.%) and SLE ($C_{\text{Friedelin}}$ = 24.0 wt.%) with dichloromethane. The argument is even more pertinent for ethanol extractions, where $C_{\text{Friedelin}}$ values of 6.2-6.5 wt.% were attained. These reinforce the greater abundance of polar compounds in this biomass. On the other hand, it is also worth noting that values of $C_{\text{Friedelin}}$ above 30 wt.% can be achieved by SFE for several combinations of operating conditions (*i.e.,* different temperatures, CO_2 flow rates, and ethanol content) as evidenced by runs SFE1-SFE3, SFE5, SFE10-SFE12, and SFE15 (see Table 2).

Finally, the selectivity towards friedelin ($\alpha_{\text{F,nF}}$) ranged from 1.1 in run SFE7 [50 ℃, 2.5 wt.% EtOH, 8 $g_{CO_2}\text{min}^{-1}$] to 3.1 in run SFE11 [50 ℃, 5 wt.% EtOH, 11 $g_{CO_2}\text{min}^{-1}$]. In fact, it is crucial to emphasize that all $\alpha_{\text{F,nF}}$ values scored higher than 1.0 and that the maximum selectivity attained is higher than the selectivities reported by Melo *et al.* [13]

for an extraction time of 6 h, which emphasizes even more the relevance of process optimization.

3.2 Statistical modeling and optimization

To compare the impact of the studied factors and their interactions on the responses, Pareto charts of the linear, quadratic and crossed effects are presented in Figure 3. The black and white colors indicate the type of influence (numerically positive or negative, respectively) of each factor/interaction. Effects whose bars are shorter than the statistical significance line (red vertical line) can be considered non-significant for a confidence level of 95 % (η_{Total}) or 90 % ($C_{\mathrm{Friedelin}}$ or $\alpha_{\mathrm{F,nF}}$). It is worth noting that initially both $C_{\mathrm{Friedelin}}$ and $\alpha_{\mathrm{F,nF}}$ were tested for a 95 % confidence level but the effect bars were all positioned below the statistical significance threshold. This is a consequence of the more balanced distribution of the effects on those responses (see Figures 3b and 3c), which hinders the existence of isolated influential factors or interactions for a stricter confidence level (such as in the case of η_{Total}, see Figure 3a). The said balance on effects magnitude was also observed by Cossuta et al. [24] for SFE of sea buckthorn (*Hippophae rhamnoides* L.) pomace, and by Oliveira et al. [25] for SFE of Brazilian cherry (*Eugenia uniflora* L.). On the other hand, a common feature of all Pareto charts is the prevalence of positive effects (in comparison to negative ones), which is in agreement with the experimental observations (see Table 2).

In terms of total yield (Figure 3a) the three individual factors ($T, EtOH, Q_{\mathrm{CO_2}}$) stand out as the most significant effects all with a linear positive impact on η_{Total}. Among these, EtOH content is by far the most influential parameter causing stronger enhancements of η_{Total} when increased. This behavior emphasizes the important role played by the

cosolvent due to the polarity modification imparted to SC-CO_2. In turn, the second most influent factor is Q_{CO_2} with an effect scoring *ca*. 42.6 % lower than EtOH in terms of importance. In any case, an increase of the CO_2 flow rate (*e.g.,* from 5 to 11 g min^{-1}) is able to improve η_{Total} as illustrated in Table 2. This is certainly due to the film resistance to mass transfer that may prevail at lower flow rates and thus decrease the extraction rate. Similar results were observed for SFE of *E. globulus* bark particles (size < 2 mm) where a significant rate improvement was attained by changing Q_{CO_2} from 6 to 12 g min^{-1} but not from 12 to 14 g min^{-1} [10,26]. Additionally, for lower Q_{CO_2} the accumulation of solutes in the fluid phase inside the extractor may decrease the driving force for mass transfer.

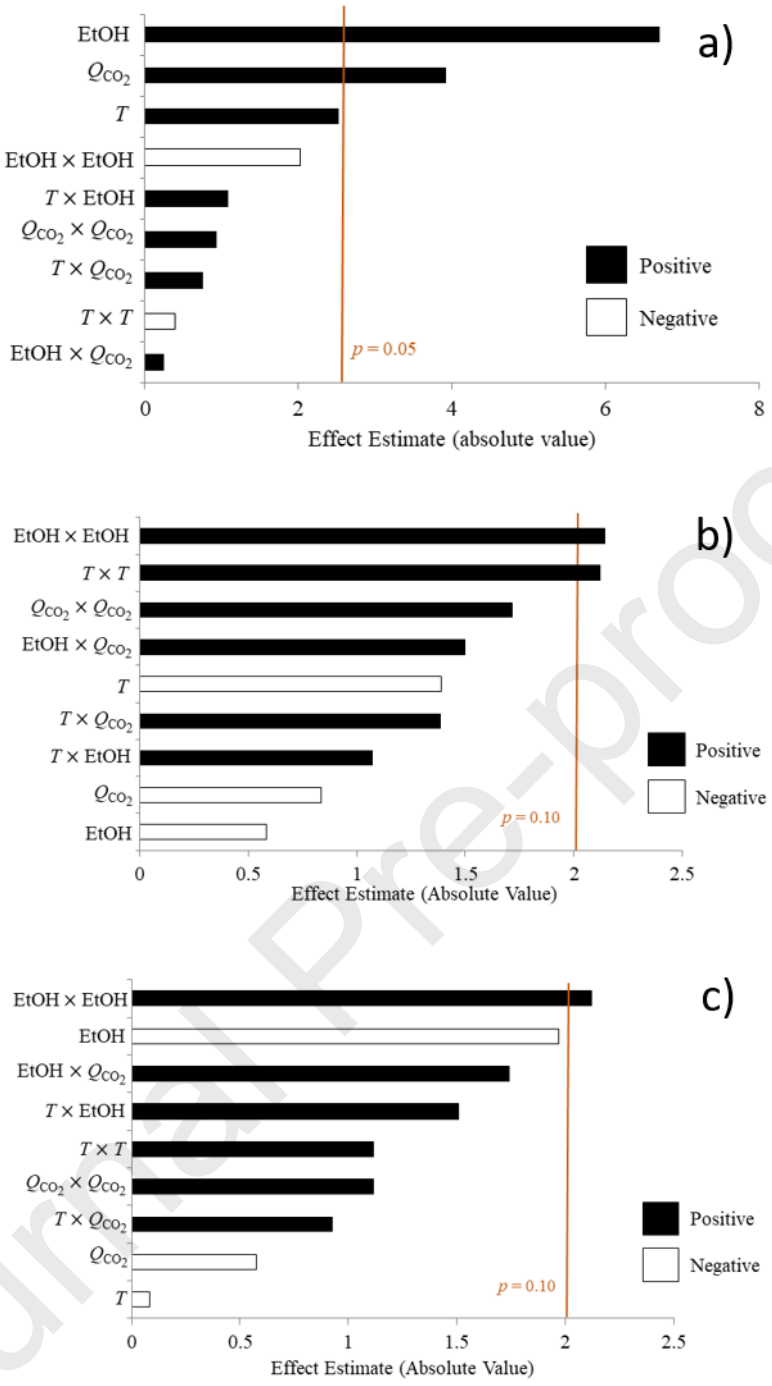

Figure 3 – Pareto charts for SFE of *Q. cerris* cork showing the influence of the factors on the responses: (a) η_{Total}, (b) $C_{\text{Friedelin}}$, and (c) $\alpha_{\text{F,nF}}$.

Regarding temperature, T, its effect bar lies in the vicinity of the statistically significant exclusion limit with p = 0.053 (for 95 % confidence level). From a thermodynamic point of view, an increment of T has two opposing effects in supercritical fluids: it reduces the solvent power through density reduction and, on the other hand, it enhances

solubility by increasing the vapor pressure of the solutes (friedelin and others) [5,10,14,27]. Remarkably, within the range of our experimental conditions a positive impact of T was observed, which means that vapor pressure growth prevailed over density reduction. For example, η_{Total} increased 46.7 % when T increased from 40 to 60 ℃, under fixed $Q_{\mathrm{CO_2}}$ and EtOH content (SFE4 and SFE15). This result clearly differs from studies reported for other species where lower temperatures led to higher η_{Total} [15,17].

In terms of $C_{\mathrm{Friedelin}}$ (Figure 3b), the quadratic effect of ethanol content (EtOH×EtOH) and temperature (T×T) scored both as positive and as the most significant effects. An important result in this graph is the non-observance of the Pareto principle in the sorting of the effects (*i.e.*, 20/80 rule). Instead, a step like arrangement of the bars is observed with individual magnitudes of the bars not exceeding 2.5 units (contrarily to the Pareto plot for η_{Total} - see Figure 3a). This substantiates the need to consider a 90 % confidence level to ensure statistical significance of the effects for the response $C_{\mathrm{Friedelin}}$. The positive sign of all quadratic effects suggests that non-linear jumps might be expected and that a region of minimum $C_{\mathrm{Friedelin}}$ may appear. Furthermore, the combined effect of CO_2 flow rate with ethanol content or temperature ($\mathrm{EtOH} \times Q_{\mathrm{CO_2}}$ or $T \times Q_{\mathrm{CO_2}}$) contributes also with a positive synergy to $C_{\mathrm{Friedelin}}$ values.

The Pareto chart (Figure 3c) for selectivity towards friedelin allows a direct insight on the great influence of ethanol as cosolvent. In fact, the effects involving EtOH were ranked on top and mainly with a positive contribution to $\alpha_{\mathrm{F,nF}}$. Nonetheless, only the quadratic term of cosolvent content (EtOH×EtOH) was deemed significant suggesting that modification of polarity of the supercritical phase leads to favorable but non-linear selectivity profiles along the ethanol content range of 0 and 5 wt.%.

In what concerns regression modeling of the three responses (η_{Total} , $C_{\text{Friedelin}}$ and $\alpha_{\text{F,nF}}$), the data from Table 2 were coded according to Eq. (6) and submitted to RSM analysis to obtain the individual and crossed coefficients of Eq. (7). These coefficients are listed in Table 3, where the bold values indicate statistically significant coefficients.

For total extraction yield the results are in accordance with the information given by the Pareto diagram (Figure 3a): only four parameters can be considered statistically significant, namely β_0, β_1, β_2 and β_3, which correspond to the constant of the polynomial model (Eq. (7)) and to the linear effects of T, EtOH and Q_{CO_2}, respectively. Between full and reduced model the fitting AARD score increases from 7.2 and 11.1 % (see Table 4), but the latter falls still below the experimental errors determined between the replicates (SFE7 to SFE9), which is worth 12.1 %.

For $C_{\text{Friedelin}}$ and $\alpha_{\text{F,nF}}$ the results are also in agreement with the information evidenced by the Pareto charts (Figures 3b and 3c, respectively). Nevertheless, to ensure a reasonable goodness of fit for optimization purposes the non-significant contributions of $Q_{\text{CO}_2} \times Q_{\text{CO}_2}$, $\text{EtOH} \times Q_{\text{CO}_2}$, T and $T \times Q_{\text{CO}_2}$ (all with effect estimates above 1.4 units, see Figure 3b) were maintained to fit the $C_{\text{Friedelin}}$ response surface model. An analogous strategy was adopted for $\alpha_{\text{F,nF}}$. This approach gives a pronounced gap between the values of R^2 and R^2_{adj} (sensitive to excess of parameters) as shown in Table 4 for the full models (FM), particularly for $C_{\text{Friedelin}}$ and $\alpha_{\text{F,nF}}$. However, the fitting AARD values are very good in both of these cases, scoring only 3.9-4.1 % for $C_{\text{Friedelin}}$ models, and bit higher for $\alpha_{\text{F,nF}}$, namely 10.6-12.1 % (see Table 4). Once again, these errors are lower than the respective experimental errors for each response, amounting 7.0 % for $C_{\text{Friedelin}}$, and 15.4 % for $\alpha_{\text{F,nF}}$.

The reduced models (RM) were refitted to the data and then converted to uncoded variables by substitution of Eq. (6) in the respective terms of Eq. (7). The final expressions for each response are the following:

$$\eta_{\text{Total}} = -0.6038 + 0.0165\,T + 0.1755\,\text{EtOH} + 0.085417\,Q_{CO_2} \quad (11)$$

$$C_{\text{Friedelin}} = 136.026 - 2.994\,T + 0.0247\,T^2 - 3.783\,\text{EtOH} + 0.399\,\text{EtOH}^2 - 6.690\,Q_{CO_2} + 0.222 Q_{CO_2}{}^2 + 0.0517\,T \times Q_{CO_2} + 0.223\text{EtOH} \times Q_{CO_2} \quad (12)$$

$$\alpha_{\text{F,nF}} = 12.128 - 0.282\,T + 0.0025\,T^2 - 1.310\,\text{EtOH} + 0.076\,\text{EtOH}^2 - 0.569\,Q_{CO_2} + 0.028 Q_{CO_2}{}^2 + 0.013\,T \times Q_{CO_2} + 0.05\text{EtOH} \times Q_{CO_2} \quad (13)$$

3.2.1 Total extraction yield response

Response surfaces for η_{Total} (Eq. (10)) are shown in Figure 4, plotting the effect of T and Q_{CO_2} for 5 wt.% EtOH (Figure 4a) and the effect of EtOH and Q_{CO_2} at 50 ºC (Figure 4b). Starting with Figure 4a, it is perceptible how an increase of Q_{CO_2} has a slightly stronger impact (*i.e.,* larger slope) on η_{Total} when compared with T. Hence, when both factors are simultaneously increased to their maximum values (11 $g_{CO_2}\text{min}^{-1}$ and 60 ºC), a positive synergy may be expected leading to the highest yield (η_{Total} = 2.3 wt.%). In turn, Figure 4b (with T = 50 ºC) shows a surface with a bigger slope (comparing with Figure 4a), which stresses the major impact of cosolvent content on the η_{Total} response. For the lowest values of these two operating conditions (*i.e.*, 0 wt.% EtOH and 5 $g_{CO_2}\text{min}^{-1}$) the model predicts correctly the smallest η_{Total} in agreement with the experimental data (SFE5). Furthermore, with high ethanol content (*i.e.,* 5.0 wt.%) and low Q_{CO_2} one can obtain greater yields than when Q_{CO_2} is high and EtOH is low (0 wt.%), which reiterates the coherency of the individual effects seen in the Pareto chart (Figure 3a).

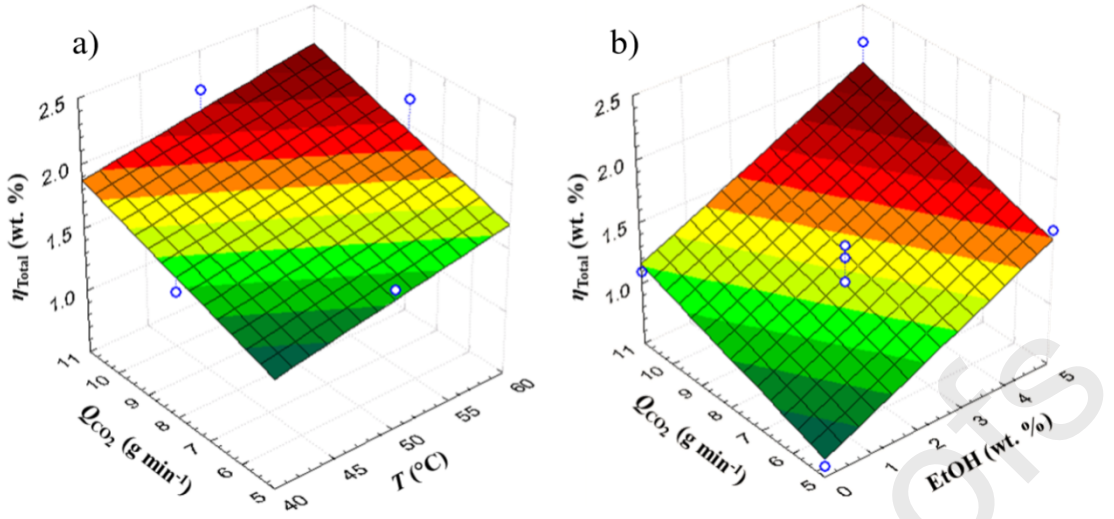

Figure 4 – Response surfaces for total extraction yield (η_{Total}) as function of: (a) T and $Q_{\mathrm{CO_2}}$, for 5 wt.% EtOH content, and (b) EtOH and $Q_{\mathrm{CO_2}}$, at 50 °C. Dots represent experimental data and the response surfaces are given by Eq. (10).

3.2.2. Friedelin concentration response

Response surfaces for $C_{\mathrm{Friedelin}}$ (Eq. (11)) as function of two parameters are shown in Figure 5a (for 5 wt.% EtOH) and Figure 5b (at 50 ºC). Although represented for the same set of independent variables and conditions, these plots are rather different from those presented for η_{Total} (Figure 4). Furthermore, the poor fitting quality can be assessed visually with some data points lying farther from the predicted values ($R^2 =$ 0.697), which means that conclusions about friedelin concentration can be drawn from the model but also contrasted with experimental data. This is the reason why additional experiments have been carried out as discussed below (Section 3.3).

In Figure 5a, (for 5 wt.% EtOH) high T and low $Q_{\mathrm{CO_2}}$ lead to a region of low $C_{\mathrm{Friedelin}}$ (*ca.* 29 wt.%). In contrast, high $C_{\mathrm{Friedelin}}$ is predicted for the combination of high T and high $Q_{\mathrm{CO_2}}$, which agrees with the positive synergy of these combined factors in the Pareto chart (Figure 3b). Furthermore, Figure 5b displays the positive effect of EtOH

and Q_{CO_2} at 50 °C, with the model estimating high $C_{Friedelin}$ in two situations: (i) when EtOH and Q_{CO_2} are both at their maximum (*i.e.,* 5 wt.% and 11 $g_{CO_2}min^{-1}$), or (ii) when EtOH and Q_{CO_2} are both at their minimum values (*i.e.,* 0 wt.% and 5 $g_{CO_2}min^{-1}$).

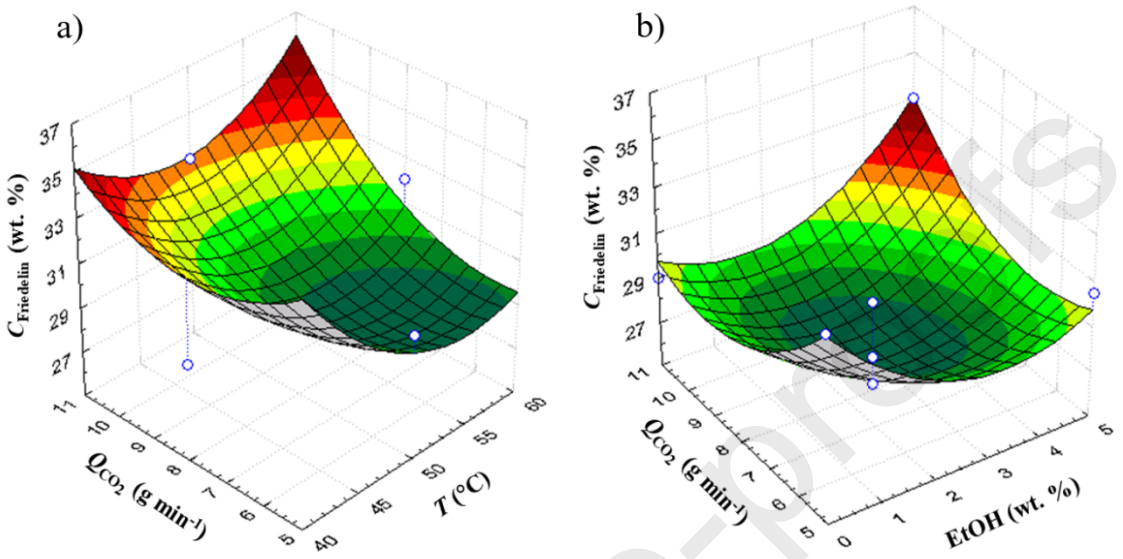

Figure 5 - Response surfaces for friedelin concentration ($C_{Friedelin}$) as function of (a) T and Q_{CO_2}, for 5 wt.% EtOH content, and (b) EtOH and Q_{CO_2}, at 50 °C. Dots represent experimental data and the response surfaces are given by Eq. (11).

According to the reduced model (Table 4), the operating conditions that numerically provide maximum $C_{Friedelin}$ in *Q. cerris* extracts (*i.e.*, 38.2 wt.%) are the combination of a low T (40 °C) and low Q_{CO_2} (5 g min^{-1}) without cosolvent addition (0 wt.% EtOH). This is a remarkable example showing that the most aggressive SFE conditions might not lead to better performances, particularly if the responses depend on specific thermodynamic trade-offs. A similar trend has been reported for the concentration of diterpenes in extracts produced by SFE of spent coffee grounds [17].

3.2.3. Selectivity to friedelin response

The response surfaces for the selectivity to friedelin ($\alpha_{F,nF}$) are presented in Figure 6 for fixed ethanol content (5 wt.%, Figure 6a) and fixed temperature (50 ℃, Figure 6b). The experimental and predicted $\alpha_{F,nF}$ datapoints are close, and the goodness of fit (R^2 = 0.713) is similar to that for $C_{Friedelin}$ (R^2 = 0.697). Therefore, identical caution is recommended as in the case of $C_{Friedelin}$, *i.e.* the modeling results should be crossed with the experimental data notwithstanding the modeled and experimental selectivity trends are totally coherent. In any case, additional assays were carried out as mentioned above. The RSM model predicts $\alpha_{F,nF} > 1.0$, within the full experimental space covered by the DoE, which means that friedelin can be extracted selectively regardless of the SFE operating conditions.

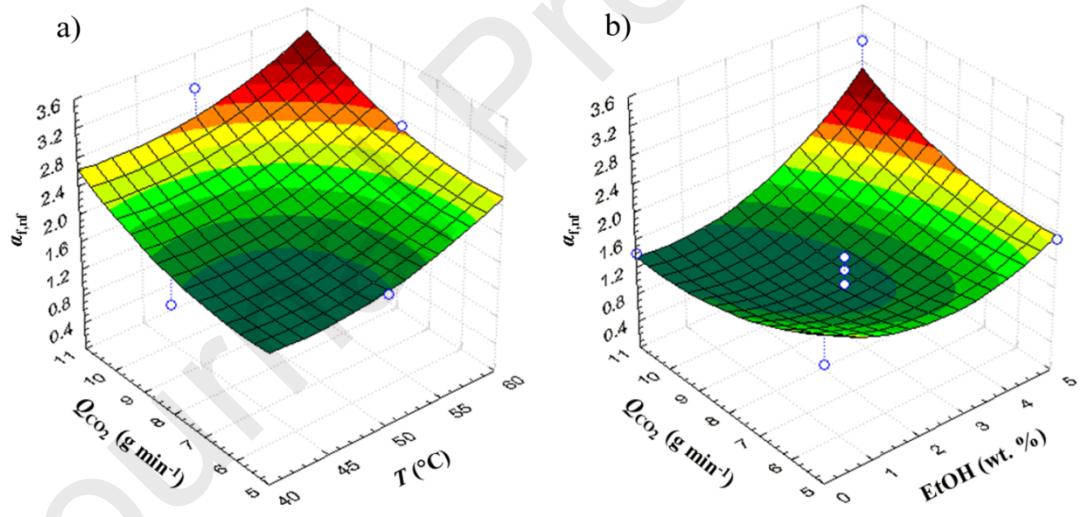

Figure 6 – Response surfaces for selectivity towards friedelin ($\alpha_{F,nF}$) as function of: (a) T and Q_{CO_2}, for 5 wt.% EtOH content; (b) EtOH and Q_{CO_2}, at 50 ℃. Dots represent experimental data and the response surfaces are given by Eq. (12).

The synergy effect of T and Q_{CO_2} can be visualized in Figure 6a and is coherent with the insights from the respective Pareto chart (Figure 3c). Accordingly, increasing both

factors simultaneously leads to a remarkably high selectivity ($\alpha_{F,nF}$ = 3.1, predicted with Eq. (12)), with the maxima region (*i.e.,* $\alpha_{F,nF}$ > 2.6) comprising a space triangle whose (Q_{CO_2},T) vertices are *ca.* (11,47), (11,60) and (8,60) in $(\text{g min}^{-1},℃)$ units.

Moreover, Figure 6b highlights the impact of ethanol on selectivity tuning. For instance, selectivity increases *ca*. 93 % ($\alpha_{F,nF}$ goes from 1.4 to 2.7) when $Q_{CO_2} = 11\ \text{g min}^{-1}$ and the ethanol content increases from 0 to 5 wt.%. In turn, at lower CO_2 flow rates the same increment of EtOH content induces moderate but still advantageous gains of $\alpha_{F,nF}$. This positive effect of ethanol on friedelin selectivity was previously reported for SFE with extraction time of 6 h [13] but the study pointed to 2.5 wt.% EtOH as the most favorable content. In the present study, $\alpha_{F,nF}$ reached 3.3 with 5.0 wt.% EtOH and $Q_{CO_2} = 11\ \text{g min}^{-1}$, $T = 60$ ºC and t = 8.0 h. Once again, these results point out the importance of SFE operating conditions optimization.

3.3 SFE experiments at optimized operating conditions

The fitted reduced models given by Eqs. (11)-(13) were used to search the operating conditions that maximize the respective response and the obtained results are listed in Table 5.

With reference to η_{Total}, the optimum occurs for maximum temperature (60 ºC), ethanol content (5 wt.%) and CO_2 flow rate (11 g min^{-1}). For this set of conditions (not included in the experimental plan of the Box-Behnken design) the estimated results are: η_{Total} = 2.2 wt.%, $C_{Friedelin}$ = 36.0 wt.%, and $\alpha_{F,nF}$ = 3.3. Remarkably, the optimum for η_{Total} coincide with the optimum conditions for enhanced selectivity towards friedelin. This is an interesting situation in the sense that $\alpha_{f,nf}$ is rarely computed in SFE studies and optimization is often driven merely by the bulk extract production, *i.e.* η_{Total}.

On the other hand, the preferable conditions for maximum $C_{\text{Friedelin}}$ are considerably distinct, namely: 40 °C, 0 wt.% EtOH and 5 $g_{CO_2}\,min^{-1}$. The calculated friedelin concentration in the extracts is 38.2 wt.%, which is only 1.06 times higher than the value obtained for the other optimum conditions (see Table 5). At the same time, under the best conditions for the friedelin concentration, η_{Total} and $\alpha_{\text{f,nf}}$ decrease 78 % and 15 % in relation to their own optimum. Hence, despite the industrial preference to operate at low temperature (40 ºC) and without cosolvent (0 wt.% EtOH), the optimum conditions for $C_{\text{Friedelin}}$ impose a heavy penalty on total extraction yield and on selectivity while its incremental gain is very small (from 36.0 to only 38.2 wt.%). For this reason, experimental confirmation of the predicted responses was performed for the optimum conditions for η_{Total} and $\alpha_{\text{F,nF}}$.

An additional experiment (SFE16) to validate the model was performed at 60 ºC with 5 wt.% EtOH and 11 $g_{CO_2}\,min^{-1}$, which represents a special vertex of the cubic experimental space considered. The SFE16 results were the following: η_{Total} = 2.4 wt.%, $C_{\text{Friedelin}}$ = 27.4 wt.% and $\alpha_{\text{F,nF}}$ = 1.7. The experimental total extraction yield is slightly higher than the estimated value (2.2 wt.%) and the other responses are substantially lower. The underestimation of η_{Total} at the optimum conditions is in agreement with a previously observed underrating tendency of the RSM model in that experimental region (see Figure 4a), but the prediction error is only 9.0 % while the computed AARD of the reduced model is 11.1 % (see Table 4). In turn, the higher deviations of the predicted *versus* experimental results for $C_{\text{Friedelin}}$ (36.0 *vs.* 27.4) and $\alpha_{\text{F,nF}}$ (3.3 *vs.* 1.7) largely exceed the AARD values of the respective reduced RSM models, and are in agreement with the inferior adjusted coefficients of determination of both models to represent the experimental data, as has been discussed above.

An additional assay (SFE17) was performed to assess the impact of cosolvent addition. Using 20 wt.% EtOH, 11 g_{CO_2} min^{-1} and 60 ºC provided a total extraction yield of 4.6 wt.%, which is much higher than η_{Total} for SFE16 (with 5 wt.% EtOH) and even higher than the reference value obtained by Soxhlet extraction (η_{Total}= 4.3 wt.%, Table 2).

In terms of $C_{\text{Friedelin}}$, SFE16 and SFE17 assays confirmed the negative effect of ethanol content, as values of 22.2 wt.% for run SFE17 (with 20 wt.% EtOH) and 27.4 wt.% for run SFE16 (with 5 wt.% EtOH) were attained. The friedelin content in run SFE17 was the lowest result of this study but the specific friedelin yield from biomass ($\eta_{\text{Total}} \times C_{\text{Friedelin}}$) was higher for SFE17 (1.02 wt.%) than for SFE16 (0.66 wt.%) although slightly lower than in the Soxhlet extraction (1.05 wt.%).

These results are in agreement with the insights reported recently by Vieira et al [30] for the same biomass, who studied the friedelin removal using methanol or ethanol as solvents in batch solid-liquid or Soxhlet extraction. Accordingly, they demonstrated that the straightforward use of these polar solvents move away the composition of the global extracts from those of pure friedelin, at the expenses of the uptake of other types of molecules. At the same time, the opposite effect (*i.e.,* approximation to pure friedelin) was observed when using petroleum ether or dichloromethane either in SLE or Soxhlet extraction. Overall, our results suggest that high concentrations of ethanol enhance the affinity of the supercritical fluid to more polar species such as phenolic compounds [28] or glycosides [29], thus increasing the total yield (from SFE16 to SFE 17 the total yield almost duplicates) but the ensuing extracts have a lower content of the target molecule (friedelin).

4. Conclusions

The effects of temperature (T, 40-60 ℃), ethanol content (EtOH, 0-5 wt.%) and CO_2 flow rate (Q_{CO_2}, 5-11 g min^{-1}) on the supercritical fluid extraction (SFE) of *Quercus cerris* cork were investigated using a Box-Behnken design of experiments and response surface methodology (RSM). The studied responses were total extraction yield (η_{Total}), friedelin concentration in the extracts ($C_{Friedelin}$) and selectivity to friedelin ($\alpha_{F,nF}$).

The fitted RSM model for η_{Total} estimated a maximum yield of 2.2 wt.% to occur for the combination of maximum T, EtOH, Q_{CO_2} (60 ℃, 5.0 wt.%, 11 g_{CO_2} min^{-1}). At the same time, the $\alpha_{F,nF}$ response scored above 1.0 within the whole experimental space studied, thus reinforcing SFE as a strong technology for the selective uptake of friedelin from *Q. cerris* cork. An additional assay with 20 wt.% EtOH (T = 60 ℃, Q_{CO_2}= 11 g_{CO_2} min^{-1}) showed opposing effects caused by the use of cosolvent, *i.e.* it increases the yield (η_{Total} = 4.6 wt.%) but lowers the concentration of the target molecule ($C_{Friedelin}$= 22.2 wt.%).

Overall, the prevailing optimum conditions for the studied SFE process will depend on the ultimate goal of the SFE process: quantity (η_{Total}) or quality ($C_{Friedelin}$) of the extract.

4. Acknowlegements

This work was developed within the scope of the project CICECO-Aveiro Institute of Materials, FCT Ref. UID/CTM/50011/2019, financed by national funds through the FCT/MCTES. Authors want to thank the funding from Project AgroForWealth (CENTRO-01-0145-FEDER-000001), funded by Centro2020, through FEDER and PT2020.

5. References

[1] S. Silva, M. Sabino, E. Fernandes, V. Correlo, L. Boesel, R.L. Reis, Cork: properties, capabilities and applications, International Materials Review. 53 (2008) 256.

[2] H. Pereira, Cork: Biology, Production and Uses, Elsevier B.V., Amesterdam, 2007.

[3] C.B. Lopes, J.R. Oliveira, L.S. Rocha, D.S. Tavares, C.M. Silva, S.P. Silva, N. Hartog, A.C. Duarte, E. Pereira, Cork stoppers as an effective sorbent for water treatment: The removal of mercury at environmentally relevant concentrations and conditions, Environmental Science and Pollution Research. 21 (2014) 2108–2121.

[4] I.M. Aroso, A.R. Araújo, R.A. Pires, R.L. Reis, Cork: Current Technological Developments and Future Perspectives for this Natural, Renewable, and Sustainable Material, ACS Sustainable Chemistry and Engineering. 5 (2017) 11130–11146.

[5] A. Şen, M.M.R. de Melo, A.J.D. Silvestre, H. Pereira, C.M. Silva, Prospective pathway for a green and enhanced friedelin production through supercritical fluid extraction of *Quercus cerris* cork, The Journal of Supercritical Fluids. 97 (2015) 247–255.

[6] C. Sunil, V. Duraipandiyan, S. Ignacimuthu, N.A. Al-Dhabi, Antioxidant, free radical scavenging and liver protective effects of friedelin isolated from *Azima tetracantha* Lam. leaves, Food Chemistry. 139 (2013) 860–865.

[7] P. Antonisamy, V. Duraipandiyan, S. Ignacimuthu, Anti-inflammatory, analgesic and antipyretic effects of friedelin isolated from *Azima tetracantha* Lam. in mouse and rat models, Journal of Pharmacy and Pharmacology. 63 (2011) 1070–1077.

[8] B. Lu, L. Liu, X. Zhen, X. Wu, Y. Zhang, Anti-tumor activity of triterpenoid-rich extract from bamboo shavings (Caulis bamfusae in Taeniam), African Journal of Biotechnology, 9 (2010) 6430–6436.

[9] R.A.R. Pires, S.P.A.S.. Martins, J.A.M. Chagas, R.L.G. Reis, Extraction and purification of friedelin, EP2070906A1.

[10] M.M.R. de Melo, A.J.D. Silvestre, C.M. Silva, Supercritical fluid extraction of vegetable matrices: Applications, trends and future perspectives of a convincing green technology, Journal of Supercritical Fluids. 92 (2014) 115–176.

[11] S. Zhao, D. Zhang, Supercritical fluid extraction and characterisation of *Moringa oleifera* leaves oil, Separation and Purification Technology. 118 (2013) 497–502.

[12] J.Z. Yin, A.Q. Wang, W. Wei, Y. Liu, W.H. Shi, Analysis of the operation conditions for supercritical fluid extraction of seed oil, Separation and Purification Technology. 43 (2005) 163–167.

[13] M.M.R. de Melo, A. Şen, A.J.D. Silvestre, H. Pereira, C.M. Silva, Experimental and modeling study of supercritical CO_2 extraction of *Quercus cerris* cork: Influence of ethanol and particle size on extraction kinetics and selectivity to friedelin, Separation and Purification Technology. 187 (2017).

[14] M.M.R. de Melo, E.L.G. Oliveira, A.J.D. Silvestre, C.M. Silva, Supercritical fluid extraction of triterpenic acids from *Eucalyptus globulus* bark, The Journal of Supercritical Fluids. 70 (2012) 137–145.

[15] R.M.A. Domingues, M.M.R. De Melo, E.L.G. Oliveira, C.P. Neto, A.J.D. Silvestre, C.M. Silva, Optimization of the supercritical fluid extraction of triterpenic acids from *Eucalyptus globulus* bark using experimental design, Journal of Supercritical Fluids. 74 (2013).

[16] D. Bas, I.H. Boyaci, Modeling and optimization I: Usability of response surface methodology, Journal of Food Engineering. 78 (2007) 836–845.

[17] H.M.A. Barbosa, M.M.R. de Melo, M.A. Coimbra, C.P. Passos, C.M. Silva, Optimization of the supercritical fluid coextraction of oil and diterpenes from spent coffee grounds using experimental design and response surface methodology, Journal of Supercritical Fluids. 85 (2014) 165–172.

[18] C. Da Porto, D. Voinovich, D. Decorti, A. Natolino, Response surface optimization of hemp seed (*Cannabis sativa* L.) oil yield and oxidation stability by supercritical carbon dioxide extraction, Journal of Supercritical Fluids. 68 (2012) 45–51.

[19] K. Zaghdoudi, X. Framboisier, C. Frochot, R. Vanderesse, D. Barth, J. Kalthoum-Cherif, et al., Response surface methodology applied to Supercritical Fluid Extraction (SFE) of carotenoids from Persimmon (*Diospyros kaki* L.), Food Chemistry. 208 (2016) 209–219.

[20] E.L.C. Cheah, P.W.S. Heng, L.W. Chan, Optimization of supercritical fluid extraction and pressurized liquid extraction of active principles from *Magnolia officinalis* using the Taguchi design, Separation and Purification Technology. 71 (2010) 293–301.

[21] L.S. Kassama, J. Shi, G.S. Mittal, Optimization of supercritical fluid extraction of lycopene from tomato skin with central composite rotatable design model, Separation and Purification Technology. 60 (2008) 278–284.

[22] B. Liu, B. Shen, F. Guo, Y. Chang, Optimization of supercritical fluid extraction of dl-tetrahydropalmatine from rhizome of *Corydalis yanhusuo* W.T. Wang with orthogonal array design, Separation and Purification Technology. 64 (2008) 242–246.

[23] D.C. Montgomery, Design and Analysis of Experiments, John Wiley & Sons, Inc., 6th Ed.,USA, 2006.

[24] D. Cossuta, B. Simándi, J. Hohmann, F. Doleschall, T. Keve, Supercritical carbon dioxide extraction of sea buckthorn (*Hippophae rhamnoides* L.) pomace, Journal of the Science of Food and Agriculture. 87 (2007) 2472–2481.

[25] A.L. Oliveira, E.S. Kamimura, J.A. Rabi, Response surface analysis of extract yield and flavour intensity of Brazilian cherry (*Eugenia uniflora* L.) obtained by supercritical carbon dioxide extraction, Innovative Food Science and Emerging Technologies. 10 (2009) 189–194.

[26] R.M.A. Domingues, M.M.R. de Melo, C.P. Neto, A.J.D. Silvestre, C.M. Silva, Measurement and modeling of supercritical fluid extraction curves of *Eucalyptus globulus* bark: Influence of the operating conditions upon yields and extract composition, Journal of Supercritical Fluids. 72 (2012) 176–185.

[27] M.M.R. de Melo, I. Portugal, A.J.D. Silvestre, C.M. Silva, Environmentally benign supercritical fluid extraction, in: M.T. Francisco Pena-Pereira (Ed.), The Application of Green Solvents in Separation Processes, Elsevier, 2017.

[28] S.A.O. Santos, J.J. Villaverde, C.M. Silva, C.P. Neto, A.J.D. Silvestre, Supercritical fluid extraction of phenolic compounds from *Eucalyptus globulus* Labill bark, Journal of Supercritical Fluids. 71 (2012) 71–79.

[29] K. Ameer, B.-S. Chun, J.-H. Kwon, Optimization of supercritical fluid extraction of steviol glycosides and total phenolic content from *Stevia rebaudiana (*Bertoni) leaves using response surface methodology and artificial neural network modeling, Industrial Crops and Products. 109 (2017) 672–685.

[30] P.G. Vieira, M.M.R. de Melo, A. Şen, M.M.Q. Simões, I. Portugal, H. Pereira, C.M. Silva, *Quercus cerris* extracts obtained by distinct separation methods and solvents: Total and friedelin extraction yields, and chemical similarity analysis by multidimensional scaling, Separation and Purification Technology. 232 (2020) 115924.

[31] ChemSpider, (Accessed in November 2019). http://www.chemspider.com/.

[32] V.H. Rodrigues, M.M.R. de Melo, I. Portugal, C.M. Silva, Extraction of *Eucalyptus leaves* using solvents of distinct polarity. Cluster analysis and extracts characterization, Journal of Supercritical Fluids. 135 (2018) 263–274.

Table 1 - Selected factors (variables) and levels in codified and non-codified format.

Variable		Levels		
		Low (-1)	Medium (0)	High (+1)
x_1: Temperature (ºC)	T	40	50	60
x_2: Ethanol content (wt.%)	EtOH	0.0	2.5	5.0
x_3: CO_2 flow rate (g_{CO_2} min^{-1})	Q_{CO_2}	5	8	11

Table 2 – Experimental conditions and results for the extraction assays carried out with *Q. cerris* cork (20-40 mesh particles). The remaining conditions for the SFE runs were: pressure of 300 bar and extraction time of 8 h.

Run	T (°C)	EtOH (wt.%)	Q_{CO_2} ($g_{CO_2}min^{-1}$)	η_{Total} (wt.%)	$C_{Friedelin}$ (wt.%)	$\alpha_{F,nF}$
SFE1	40	0.0	8	1.0	34.2	2.0
SFE2	40	2.5	5	1.0	36.2	2.3
SFE3	40	2.5	11	1.3	31.3	1.8
SFE4	40	5.0	8	1.5	29.3	1.6
SFE5	50	0.0	5	0.6	33.2	1.7
SFE6	50	0.0	11	1.1	29.0	1.4
SFE7	50	2.5	8	1.3	25.3	1.1
SFE8	50	2.5	8	1.4	26.5	1.3
SFE9	50	2.5	8	1.1	29.0	1.5
SFE10	50	5.0	5	1.6	30.5	1.9
SFE11	50	5.0	11	2.2	33.0	3.1
SFE12	60	0.0	8	1.3	32.1	1.8
SFE13	60	2.5	5	1.0	28.4	1.4
SFE14	60	2.5	11	1.6	29.7	1.7
SFE15	60	5.0	8	2.2	32.0	2.7
Soxhlet extraction with dichloromethane				4.3	24.2	-
Solid-liquid extraction with dichloromethane at 23 ºC				1.5	24.0	-
Soxhlet extraction with ethanol				7.2	6.2	-
Solid-liquid extraction with ethanol at 23 ºC				2.2	6.5	-

Table 3 – Regression coefficients of the RSM polynomial given by Eq. (7) and their individual significance at 95% (η_{Total}) or 90 % ($C_{Friedelin}$ and $\alpha_{F,nF}$) confidence levels. The values in bold represent significant coefficients, and the star (*) represents coefficients retained in the reduced models.

	η_{Total}		$C_{Friedelin}$		$\alpha_{F,nF}$	
		p		p		p
β_0	1.31921*	**<0.001**	144.25509*	**<0.001**	14.62361*	**0.003**
β_1	-0.05008*	**0.053**	-3.11417*	0.223	-0.33708*	0.938
β_2	-0.20483*	**0.001**	-6.36833*	0.584	-1.31000*	**0.106**
β_3	0.12051*	**0.011**	-6.91065*	0.440	-0.87361*	0.590
β_{11}	0.00038	0.710	0.02471*	**0.087**	0.00250*	0.315
β_{22}	0.03127	0.098	0.39933*	**0.085**	0.07600*	**0.088**
β_{33}	-0.0100	0.395	0.22180*	0.147	0.02780*	0.315
β_{12}	0.0040	0.329	0.0480	0.332	0.01300	0.192
β_{13}	0.0023	0.483	0.0517*	0.224	0.00670*	0.396
β_{23}	0.0030	0.817	0.2233*	0.194	0.05000*	0.142

Table 4 – Goodness of fit indicators for the full and reduced RSM models.

Response (model)	R^2	R^2_{adj}	AARD (%)
η_{Total} (Full model)	0.937	0.822	7.2
η_{Total} (Reduced model)	0.845	0.803	11.1
$C_{Friedelin}$ (Full model)	0.789	0.262	3.9
$C_{Friedelin}$ (Reduced model)	0.697	0.152	4.1
$\alpha_{F,nF}$ (Full model)	0.768	0.188	10.6
$\alpha_{F,nF}$ (Reduced model)	0.713	0.196	12.1

Table 5 – SFE of *Q. cerris* cork: optimized operating conditions and estimated (RSM) responses at those conditions using the reduced RSM models.

Optimum Conditions for maximum	η_{Total} (wt.%)	$C_{Friedelin}$ (wt.%)	$\alpha_{F,nF}$
T (°C)	60	40	60
EtOH (wt.%)	5	0	5
Q_{CO_2} (g min $^{-1}$)	11	5	11
Estimated response at optimum conditions			
η_{Total} (wt.%)	**2.2**	0.48	2.2
$C_{Friedelin}$(wt.%)	36.0	**38.2**	36.0
$\alpha_{F,nF}$	3.3	2.8	**3.3**

LIST OF FIGURES

Figure 1 – Molecular structure of friedelin and basic physicochemical properties. Melting point: experimental database; boiling point: adapted Stein & Brown method; surface area and molar volume: ACD/Labs Percepta Platform - PhysChem Module. All data were retrieved from [31].

Figure 2 - Simplified flowsheet of the SFE unit. Retrieved from [32].

Figure 3 – Pareto charts for SFE of *Q. cerris* cork showing the influence of the factors on the responses: (a) η_{Total}, (b) $C_{\mathrm{Friedelin}}$, and (c) $\alpha_{\mathrm{F,nF}}$.

Figure 4 – Response surfaces for total extraction yield (η_{Total}) as function of: (a) T and $Q_{\mathrm{CO_2}}$, for 5 wt.% EtOH content, and (b) EtOH and $Q_{\mathrm{CO_2}}$, at 50 ℃. Dots represent experimental data and the response surfaces are given by Eq. (10).

Figure 5 - Response surfaces for friedelin concentration ($C_{\mathrm{Friedelin}}$) as function of (a) T and $Q_{\mathrm{CO_2}}$, for 5 wt.% EtOH content, and (b) EtOH and $Q_{\mathrm{CO_2}}$, at 50 ℃. Dots represent experimental data and the response surfaces are given by Eq. (11).

Figure 6 – Response surfaces for selectivity towards friedelin ($\alpha_{\mathrm{F,nF}}$) as function of: (a) T and $Q_{\mathrm{CO_2}}$, for 5 wt.% EtOH content; (b) EtOH and $Q_{\mathrm{CO_2}}$, at 50 ℃. Dots represent experimental data and the response surfaces are given by Eq. (12).

Highlights

- SFE of friedelin from *Quercus cerris* cork with pure/modified CO_2.
- Experimental conditions tested: 40–60 °C, 0–5 wt.% ethanol, 5 – 11 $g_{CO_2}\ min^{-1}$.
- Optimization of the SFE following DoE and RSM approaches.
- Total yield, friedelin concentration and selectivity to friedelin were measured.

Declaration of interests

The authors declare that they have no known competing financial interests or personal relationships that could have appeared to influence the work reported in this paper.

Carlos Manuel Silva

(Corresponding Author, on behalf of all coauthors)

Authors Statement

Marcelo M. R. de Melo: Writing - original draft; Investigation; Methodology

Pedro G. Vieira: Writing - original draft; Investigation; Methodology

Ali Şen: Investigation; Methodology; Resources

H. Pereira: Funding acquisition; Supervision

Inês Portugal: Supervision; Writing - review & editing; Conceptualization; Formal analysis

Carlos M. Silva: Funding acquisition; Supervision; Writing - review & editing; Conceptualization; Resources; Formal analysis

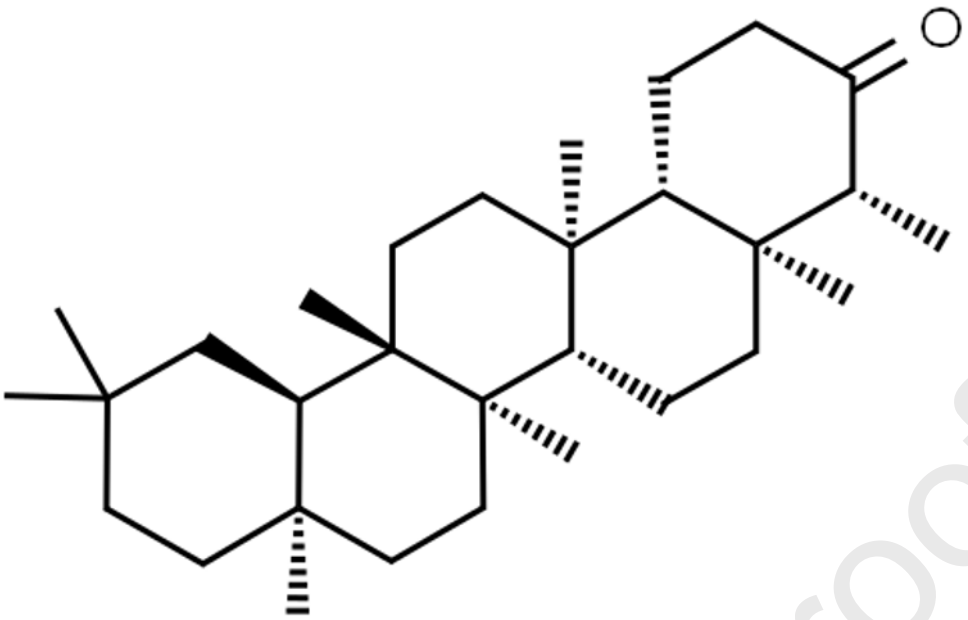

Molecular Formula:	$C_{30}H_{50}O$
Melting Point:	263 °C
Predicted Boiling Point:	447 °C
Predicted Polar Surface Area:	17 $Å^2$
Predicted Molar Volume:	443.0 ± 3.0 $cm^3\ mol^{-1}$